Available online at www.sciencedirect.com
SCIENCE DIRECT®
Journal of Power Sources 144 (2005) 494–504
JOURNAL OF POWER SOURCES
www.elsevier.com/locate/jpowsour

High-power lead–acid batteries for different applications

Rainer Wagner*

EXIDE Technologies, Deutsche EXIDE GmbH, Odertal 35, D-37431 Bad Lauterberg, Germany

Received 1 October 2004; accepted 4 November 2004
Available online 11 January 2005

Abstract

High-power lead–acid batteries have been used for a rather long time in various applications, especially for uninterruptible power supplies (UPSs) and starting of automobiles. Future automotive service requires, in addition to cold-cranking performance, the combination of high-power capability, a very good charge-acceptance, and an excellent cycle-life. Such applications include stop–start, regenerative braking, and soft, mild and full hybrid vehicles. For UPS, there has been a clear tendency to shorter discharge times and higher discharge rates. During the past decades, the specific power of lead–acid batteries has been raised steadily and there is still, room for further improvement. This paper gives an overview of the progress made in the development of high-power lead–acid batteries and focuses on stationary and automotive applications.

Keywords: Stationary batteries; Automotive batteries; High power; Copper-stretch metal; Absorptive glass mat; Spiral wound

1. Introduction

There are various applications where batteries with high discharge rate performance are required. This includes uninterruptible power supplies (UPSs) and automotive service. Despite of the rather high weight, the lead–acid battery has a relatively high specific power. Taking into account other important parameters (cost, life, reliability, possibility of recycling, availability of raw materials), the lead–acid battery is very often a suitable choice and it can be expected that this electrochemical storage system will remain an important power supply for a long time. This is especially true for stationary applications (e.g., UPS) where the high weight of lead is, in general, not so important. For such applications, volumetric power density has a higher priority than gravimetric energy density. For automotive applications, the starting of the engine requires batteries that can supply high cold-cranking currents. Future automotive service needs, in addition to the cold-cranking performance, the combination of high power capability, very good charge-acceptance and excellent cycle-life. Such applications include stop–start, regenerative braking, and soft, mild and full hybrid vehicles.

In the past decades, the specific power of lead–acid batteries has been raised steadily. These developments have also given a much better charge-acceptance. There are two ways to improve the power performance of lead–acid batteries, namely: (i) reduction of the electrical resistance of the current-collector parts, for example, the grids; (ii) optimization of grid material/design. For certain applications where cost and long service-life have lower priority, an extremely high power density has been achieved. In general, measures that improve power give lower cycling performance, and vice versa. Thus, compromises must be made. Recent developments have shown, however, that very high power can be combined with excellent cycle-life, through the adoption of novel cell designs.

2. Ways to improve power performance

The power P supplied from a battery can be expressed by the product of the discharge current I and the battery voltage U. The voltage U is the difference between the open-circuit

* Tel.: +49 231 9417310; fax: +49 231 9417311.
E-mail address: rainer.wagner@exide.de.

0378-7753/$ – see front matter © 2004 Elsevier B.V. All rights reserved.
doi:10.1016/j.jpowsour.2004.11.046

voltage (OCV), U_0 and the product IR_i, where R_i is the internal electrical resistance of the battery, i.e.,

$$P = (U_0 - IR_i) \times I \quad (1)$$

The maximum current is the short-circuit current, I_s, i.e.,

$$I_s = \frac{U_0}{R_i} \quad (2)$$

The maximum power P_{max} can be supplied at $U = 1/2U_0$, i.e.,

$$P_{max} = \frac{U_0^2}{4R_i} \quad (3)$$

Therefore, the maximum power can be raised by an increase of OCV and/or by a reduction in the internal electrical resistance.

The OCV is given mainly by the electrode couple. In case of a lead–acid battery, the OCV is around 2.15 V per cell. The exact figure depends on the concentration of sulfuric acid used as electrolyte (e.g, 2.13 V at a relative density of 1.28).

The internal electrical resistance is rather complex and does not just include a couple of ohmic resistances, but also some overpotential terms ('polarizations'). If just the specific resistance ρ of the electrolyte is considered, a power factor P_f can be calculated [1], i.e.,

$$P_f = \frac{U_0^2}{\rho} \quad (4)$$

Calculation of such a power factor for various battery types gives the best result for the lead–acid system. The reason is that the lead–acid battery has a relatively high U_0 (2.1 V) and a rather low specific resistance of sulfuric acid as the electrolyte (1.1 Ω cm). The alkaline nickel batteries (Ni–Cd or Ni–MH) have a markedly lower OCV (1.3 V) and additionally, a higher specific resistance of the electrolyte (1.8 Ω cm). Lithium-ion batteries are significantly higher in OCV (3.6 V); this is a clear advantage because the square of U_0 is taken in the power factor calculation. Organic electrolytes are used however, and have a specific resistance that is 50 times or more above that of sulfuric acid.

Double-layer capacitors, also called supercapacitors or ultracapacitors, have either aqueous electrolytes with low specific resistance, but then, U_0 cannot be much above 1 V, or organic electrolytes with much higher specific resistance so that a markedly higher U_0 is possible.

Of course, the internal electrical resistance of a battery system is not just given by the electrolyte resistance. If systems have a rather small distance between the electrodes, the effect of high specific electrolyte resistance can be compensated. The polarization effects have also to be taken into account. Supercapacitors have an extremely high electrode surface areas of more than 1000 $m^2\ g^{-1}$ and this feature can reduce markedly any polarization. It has also to be realized that sulfuric acid is a part of the electrochemical process in a lead–acid battery and is consumed during discharge, which results in increase of the specific resistance of the electrolyte. Nevertheless, the lead–acid battery has a high power capability and, in spite of the high weight of lead, should be a very suitable system for a high power supply. In addition, lead–acid has a significant cost advantage. Thus, there are numerous high-power applications where lead–acid batteries have been used.

If a bipolar design with very thin layers of positive and negative mass is used, the internal resistance will be dominated by the electrolyte resistance and then, extremely high power can be supplied but only for short periods. The life time will also be markedly reduced. Prototypes of such batteries have given about 4 $kW\ kg^{-1}$ over 10 s; this is rather impressive [1].

Most of the improvements in power capability were achieved by reduction of the internal electrical resistance. For valve-regulated lead–acid (VRLA) designs with antimony-free grid alloys, the OCV has been raised to a slightly higher level over the years by an increase in sulfuric acid concentration from a relative density of 1.26 or 1.28 to about 1.30 or even slightly higher, but there are certain limits for any further increase.

The internal electrical resistance has been reduced significantly over the past decades and there appears to be room for further reduction. As already pointed out, the internal resistance of a battery is rather complex. There is the ohmic resistance from all the current-collector parts and the electrolyte but there are also some polarization effects. The latter include charge-transfer reactions, diffusion and crystallization. All these are non-ohmic and depend significantly on the current and the time of current flow, as well as the state-of-charge (SoC) and whether the battery is on charge or discharge.

In the beginning of a high power discharge, the voltage drop mainly arises from all the ohmic resistances and the charge-transfer reaction. Very soon other effects (diffusion, change of active-mass surface) exert an influence and result in a higher voltage loss, which reduces the power capability of the battery. Thus, if very short high-power discharge pulses are required, then the polarisation is less important in comparison with a longer period of high power discharge.

3. Electric conductor parts

The ohmic resistance of the electric current conductor parts makes a significant contribution to the internal electrical resistance of the battery. It includes the grids, top bars, intercell connections, and the terminals. For high-power applications, there have been attempts to reduce the electrical resistance by improved grid designs [2,3]. This can be calculated quite readily and with high accuracy by using computers with the result that it is indeed possible to produce grid structures with markedly lower electrical resistance. Unfortunately, it is not so easy to cast well grids that have minimal electrical resistance, and this can result in higher corrosion rates. Pasting can also be more difficult. Therefore, changes in the grid

structure have to be performed carefully by considering possible casting and pasting problems [4]. A way to avoid any restrictions from grid casting was proposed recently [5]. It is a novel grid production method with an electro-deposition process, that minimizes grid weight and optimizes grid structure for low electrical resistance.

Another way to improve the high-power performance is the use of copper as the negative grid material for lead–acid batteries with high capacities and rather tall plates. The general rule is that, the taller the plates, the greater is the ratio of the grid electrical resistance to the total internal resistance of the cell. This causes, especially for plates taller than 50 cm, a lower depth-of-discharge (DoD) in the bottom regions of the cell. The large voltage drop along the grid reduces the available energy of the battery and also increases the heat generation in the cell. In order to improve this situation, a new cell type with a Copper-Stretch-Metal grid design, called CSM, was developed and placed on the market more than a decade ago [6–8]. CSM cells have the same weight and volume as the standard PzS design, but copper is used instead of lead as the negative grid material. Actually, it is an expanded copper grid covered with a thin layer of lead. On the positive side, tubular plates are used. The influence of copper as the grid material of the negative plate on the discharge and charge behaviour of the cell has been estimated by using a theoretical model developed in earlier papers [9,10]. In this model, the cell is considered as a network of vertical and horizontal resistances. A comparison of cells with plates of the same height (555 mm) shows that the CSM cell has an internal resistance, that is about 17% lower than that of the standard PzS cell. Due to the lower resistance of the negative plate, CSM displays a markedly more equalized current distribution between the top and the bottom of the cell [11]. Experimental investigations of the current distribution in CSM and standard PzS cells have confirmed the predictions obtained from the theoretical model.

The local current-density distribution of PzS and CSM cells with the same plate height (555 mm) at the beginning of a discharge at $2 \times I_5$ is shown in Fig. 1. At the top of the plates, there is a much higher current density with PzS than with CSM. Conversely, in the bottom area, the CSM cell has a higher current density than the PzS cell. This means that there is a much more equalized current distribution in CSM plates. The difference in local current density also means a difference in the local DoD of the plate. Therefore, PzS has a significant difference in mass utilization between the top and the bottom areas, especially at high discharge rates. This means that the mass utilization at the top is relatively high, while at the bottom there are mass reserves that cannot be used.

It is important to realize that the use of copper instead of lead for the negative grid is not only a benefit during discharge, but also provides a greatly improved charge-acceptance with better energy efficiency. CSM cells for traction application and OCSM cells for stationary applications should be used, where cells with tall plates, medium or high

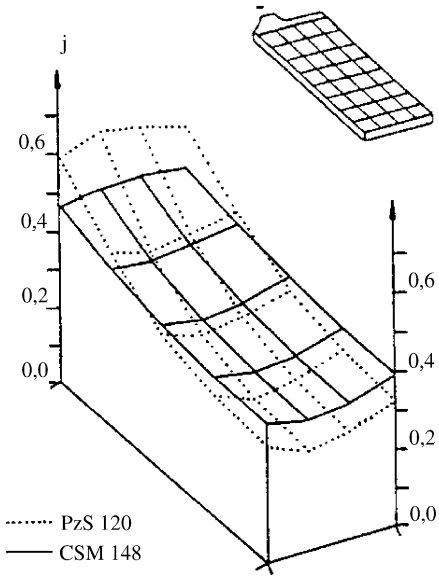

Fig. 1. Local current density distribution of standard (PzS) and CSM cells with same plate height at discharge rate of $2 \times I_5$.

discharge power, and high energy efficiency are required [6–8]. The discharge curves for a 1380-Ah OCSM cell at constant power discharges of 1.47 kW and 2.94 kW are presented in Fig. 2. The diagram also gives the discharge curves of a standard OPzS cell with the same weight and size. The much better performance of the OCSM design can be seen clearly.

OCSM cells with positive tubular plates and negative copper grids have successfully been used for various stationary applications. For example, in 1986 a 17-MW/14-MWh battery was installed at BEWAG in Berlin. At that time, the battery was the largest in the world [12–14]. Designed to strengthen Berlin's 'island' electricity supply, it was used from the beginning of 1987 for frequency regulation and spinning reserve. There were 12 battery strings in parallel and each string had 590 cells in series with a capacity of 1000 Ah. This provided, in total, a 1180-V, 12000-Ah battery that, via converters and transformers, was connected directly to the 30-kV grid of BEWAG in Berlin.

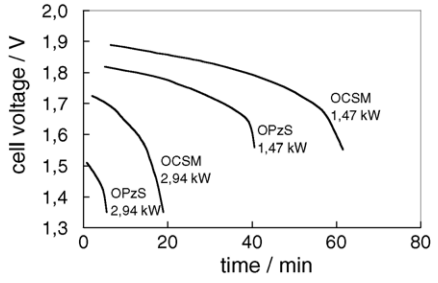

Fig. 2. Discharge curves of 1380-Ah OCSM cells composed with standard OPzS cells at high discharge rates with constant high power of 1.47 kW and 2.94 kW.

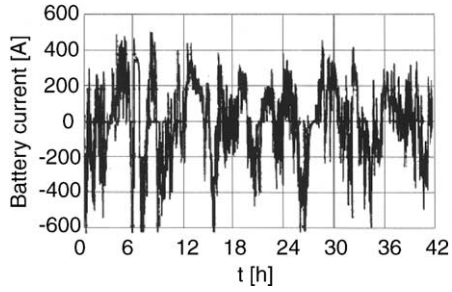

Fig. 3. Typical current flow in one battery string during frequency regulation at BEWAG.

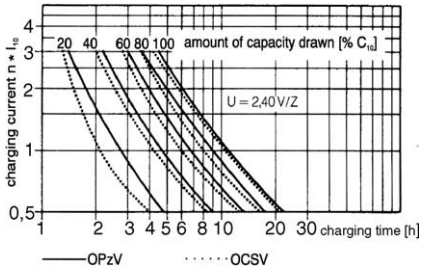

Fig. 4. Charging time and initial charging current to return a standard (OPzS) and a CSM gel (OCSV) battery to 100% of discharged capacity after discharge to different depths-of-discharge.

A typical current flow in one string of the BEWAG battery over 42 h during frequency regulation is given in Fig. 3. The current was limited to ±700 A per string. This corresponded to a maximum power of ±8.5 MW, which was sufficient to keep the frequency always at 50 Hz with a maximum deviation of ±0.2 Hz. When spinning reserve was needed, the limit of the discharge current was changed to 1400 A per string so that 17 MW were then available. In 1995, the battery reached the end of its service life. Over the whole lifetime in service, the 14 MWh battery storage system operated successfully with virtually no problems [15]. This is a very remarkable result, as the operating conditions were rather severe. The battery had a capacity turnover of some 7000 times the nominal capacity and the total energy turnover was about 100 GWh.

Large lead–acid OCSM batteries are also suitable for further utility applications. Some years ago, the concept of a multifunctional energy storage system was evaluated [16]. This system included three different functions: (i) uninterruptible power supply (UPS); (ii) improvement of power quality; (iii) peak-load shaving. Actually, nowadays, there is a growing demand for high quality power. Peak-load shaving entails the use of regenerating power sources, with the energy stored in a battery for high peak-load periods.

The use of the CSM technology for large VRLA batteries can result in high-power batteries that have all the advantages of the valve-regulated design. Till date, negative copper grids have only been used in gel cells as copper is most useful with tall plates, and in such designs gel is mostly used in order to avoid acid stratification, at least for all applications where the cells are in a vertical position. Based on a gel cell with positive tubular plates and negative lead grids (OPzV type), a new cell type called ‘OCSV’ was developed, where copper is used instead of lead as the negative grid material in a gel cell [17]. Besides higher power, such cells have also a better charge-acceptance. The charging time is given in Fig. 4 for different initial charging currents to return a standard gel cell, OPzV, and a gel cell with copper grids, OCSV to 100% of the discharged capacity. It can be seen that the use of copper grids reduces markedly the charging time due to the better charge-acceptance of the OCSV cells.

An alternative to negative copper grids is the use of a second lug (or ‘tab’) at the bottom of the plate as a current take-off tab in order to improve the current-collection function of the grid [18–20]. The benefits, especially at high discharge rates, are similar to the use of negative copper grids, namely: less voltage drop along the grid, less heat, and better and more uniform mass utilization at the bottom of the plate. Again, charge-acceptance will also be much better. The dual-tab concept has been used to develop a spiral-wound VRLA design for high-power applications.

As discussed above, a bipolar design is the best approach to minimize the electrical resistance of the conductor parts. There some reports of theoretical calculations, and about testing of prototypes made as a bipolar or a semi-bipolar version [21–25]. For short life time requirements in special applications it has proved to be quite successful. Whenever a longer life has been needed, however, such batteries have suffered from many problems as corrosion and leakage. Thus, up to now, none of these bipolar concepts have been successfully placed in the market.

4. Active mass/electrolyte

Polarization is much influenced by the surface area of the active mass. During discharge, some active mass is consumed and lead sulfate covers part of the surface. Therefore, with proceeding discharge, the available surface area is reduced significantly and this results in a steadily increasing polarization. This effect could be compensated, at least to some extent, by using an active-mass structure with higher surface area. At present, however this parameter is already on a rather high level (for the positive mass it is about $5\,m^2\,g^{-1}$) and a further increase would give a significant reduction in life time, especially in cycling applications. If life time has not a high priority, increase in surface area is a way to reduce polarization effects. It has to be realized that, during cycling, there is a marked reduction in the surface area. This ageing effect gives a decrease in the high current performance of the battery.

A good mass adhesion to the grid is important to avoid problems at the grid|mass interface. Any appearance of barrier layers results in significant increase in the electrical resistance in this part of the battery. Some decades ago, when lead–acid batteries with positive lead–calcium grids without antimony had first been placed in the market, there was a ma-

jor disaster in terms of very poor cycle-life. Investigation of the phenomenon revealed that the cause of the failure was the formation of a barrier layer of lead sulfate between the positive grid and the active mass [26–28]. The use of a proper alloy, especially with a sufficiently high tin content (often about 1 wt% or more), is important to avoid such problems [4,29–31]. A good plate processing, especially the curing, is also helpful. Both active materials (lead dioxide and lead) act as electrical conductors from the points of the electrode process to the nearest grid member. There is, however, the porous structure of the active material and the lower conductivity of lead dioxide to be considered. With proceeding discharge, steadily more lead sulfate is formed and this is non conductive. Therefore, the pellet size has an impact on the electrical resistance inside the active mass.

There has been an investigation [32] about the use of polymer-structured electrodes, where the grids were made from a polymer, coated with thin layers of copper and lead. Such grids had significantly lower weights in comparison with standard lead grids. These PNS (polymeric network structure) grids had much smaller mesh sizes than usual grids. There were some variants between 1 mm × 1 mm and 3 mm × 3 mm mesh size. It could be shown clearly that, the rather small mesh sizes gave a much better discharge performance due to the shorter current paths within the active mass. Although prototypes gave promising results, the rather high cost is a disadvantage of such electrodes.

During the discharge, sulfuric acid as the electrolyte is part of the electrochemical process and is consumed. The electrolyte inside the pores of the active mass is used first. Very soon, a diffusion starts where sulphuric acid is transferred from the space between the plates into the pores of the active mass. At high discharge rates there can be a limitation by diffusion. This results in a lack of electrolyte inside the plate, where the electrode reaction nearly stops, although there is still sufficient active mass available. A cross-section through a positive tubular plate is shown in Fig. 5. It can be seen that a 100-h discharge rate gives the same discharge level in the inner and outer parts of the plate. With a 1-h rate the inner part is just 50% discharged in comparison with the outer part due to the diffusion limitation of thick plates.

The diffusion problem can be reduced by using thinner plates. This has been a successful way in the past decades to improve automotive starter and UPS batteries. Present plates are rather thin. For certain applications, they have sometimes a thickness of just 1 mm. An alternative to a thin-plate design would be an electrolyte flow through the plates. Although a reduction of the diffusion problem could be found on tests of such prototypes, there are other disadvantages and thus, it has not been used so far in the field.

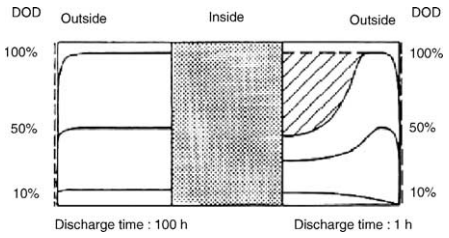

Fig. 5. Cross-section through positive tubular plate showing diffusion limitation of thick plates at high discharge rates.

The use of very thin electrodes has been reported as the TMF (thin metal foil) concept [33–35]. Spiral-round, thin, metal sheet electrodes and absorptive glass mat (AGM) separators offered extremely high power and excellent chargeability. The grids were rolled sheets of only about 0.6-mm thickness and had an active-mass layer thickness of about the same dimensions. The battery was developed for use in power tools, automobile starting and other applications where high power and rapid recharge capability is required. This development to novel design features is a good demonstration to show the extremely high power performance of the lead–acid system. It has been rather difficult however, to achieve reliability and a sufficiently long life. Another approach has been proposed recently, namely, the UHP (ultra high power) design with thin flat plates and thin microglass mats or special microporous polyethylene membranes as the separator [36]. Prototypes were tested and gave the expected improvement in power performance. Such a design is especially interesting for UPS applications.

Part of the electrolyte resistance comes from the separator. Indeed, at high discharge rates there is a significant contribution of the separator to the total voltage losses in the battery. Much progress has been made in the past decades to improve the separator with regards to many parameters that include a low electrical resistance [37,38]. Today, polyethylene separators are often used, and are made from a blend of ultrahigh-molecular-weight polyethylene pellets with a mixture of silica and oil. Such separators have a high porosity and a rather low electrical resistance. They are very useful for starter batteries where high cold-cranking performance is needed. An even lower electrical resistance can be achieved with AGM separators. This is discussed in more detail in the next section.

The effects of reduced surface area of the active mass and lack of electrolyte during longer discharge periods with high power is much influenced by the crystalline structure (porosity and crystal size) of the active mass. There is an impact from the paste recipe and density, but the manufacturing process can also exert a strong influence. This includes pasting, curing/drying, soaking, and formation. Many studies on these subjects have been published in recent years; some examples are given in [39–43]. Positive plates were made by using paste densities between 3.8 g cm^{-3} and 4.3 g cm^{-3} in combination with low, medium, and high curing temperatures, which resulted in a tribasic (3BS) or tetrabasic (4BS) lead sulfate structure of the cured mass or a mix of both [41,42]. The investigations also involved various soaking and formation programs with pulse technique and discharge steps. In the end, there were rather different crystalline structures of

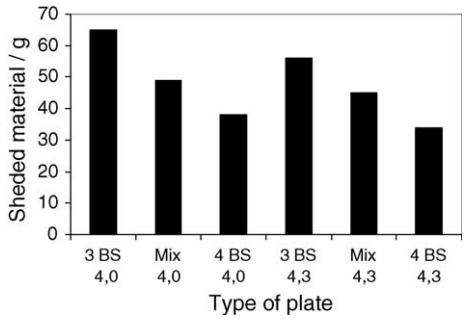

Fig. 6. Amount of positive shedded material after accelerated cycle test in a flooded system with excess of sulfuric acid and negative mass.

the formed positive mass with different initial performance data and cycle-life results.

The above studies also included an accelerated cycle test of single positive plates with an excess of electrolyte and negative mass. Different plate types were used and were made from a paste density between 3.8 g cm^{-3} and 4.3 g cm^{-3} and with cured crystalline structure of 3BS, 4BS or a mix of both. The positive plate was put between two negative counter plates in sulfuric acid with a relative density of 1.30. The discharge current was 11 A down to 1.5 V and the charge current was 2.8 A up to 2.4 V, followed by an additional charge with 0.7 A over 6 h. After 70 cycles, the test was terminated. Afterwards, the weight loss of the positive plate was measured in order to determine the amount of shedded material. The test results, are presented in Fig. 6 Plates prepared from 4BS gave less shedding than, those based on 3BS. The mix of 3BS and 4BS lies in between. There is also an influence of paste density. More shedded material was found with 4.0 in comparison with 4.3 g cm^{-3}. The accelerated cycle test with an excess of electrolyte and a high discharge rate gave comparable results with tests that employed lower discharge currents or other special cycle programs. Those tests showed that without any support of the positive active-mass, e.g., by gauntlets, as in case of tubular plates or by tight separator design, the lower porosity/higher density with more contact area between the mass particles and the better crystal network of tetrabasic lead sulphate slowed down the shedding process.

Thus, further increase of active mass porosity and surface area, as well as plate thickness reduction, has certain limits with respect to the life of the battery, especially if some cycling performance is needed. On the other hand, the use of an AGM designs with high pressure of the glass mats on the plates gives additional options. Test with the same plates used in flooded or AGM designs clearly demonstrated that with AGM, there is much better cycle-life and less influence of the cured mass structure and porosity in comparison with a flooded design. This means that with an AGM design and high pressure by glass mats, a more porous active mass and a higher surface area can be used and can result in better power capability without incurring a dramatic loss of cycling performance.

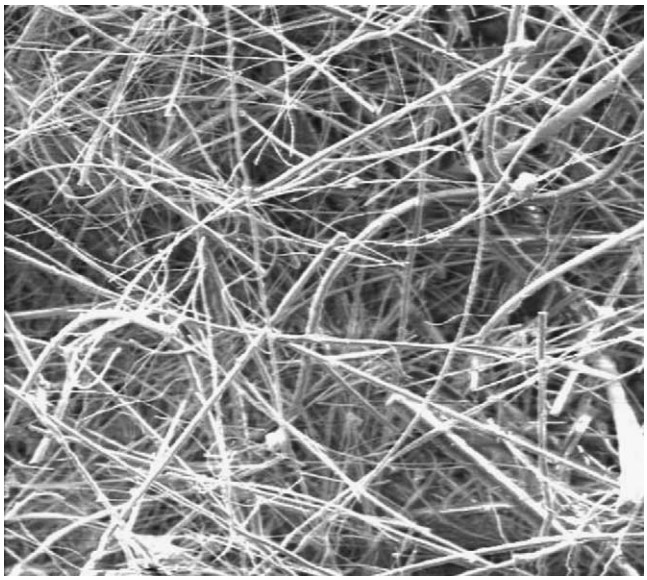

Fig. 7. Scanning electron micrograph of an AGM separator; magnification of 500×.

5. Absorptive glass mat

In AGM batteries, the electrolyte is immobilized in glass-mat separators with a very high porosity of more than 90%, a typical value is 93%. The glass fibres are rather fine and, therefore, the absorption capability is high. The medium pore-size of the glass-mat is around a few μm. An electron micrograph of a typical glass-mat separator with fine and coarse fibres, is given in Fig. 7 The interweaving glass fibres can be seen clearly.

In general, AGM batteries use positive flat plates and glass-mat separators, which are made from 100% glass fibres. Some reinforcement can be achieved with synthetic fibres in order to improve the strength of the separator [44]. Although, the 100% glass fibre version has some advantages, the mechanical properties are relatively poor, and this can be a disadvantage during plate-group assembly and for avoiding short-circuits inside the battery. As a compromise, sometimes a few percent of organic fibres are added to achieve an AGM separator with better mechanical behaviour without losing too much of the performance of the 100% pure-glass version.

The high porosity and the pore structure of the glass mat results in an extremely low electrical resistance of the separator and this makes AGM most suitable at high discharge rates. Indeed, tests with AGM and gel batteries have shown clearly that the higher the discharge rate, the better is AGM in comparison to gel. Thus, for most of the applications where high-power performance is required, AGM is used rather than the gel design [45].

For stationary applications, AGM batteries have been optimized either for life and energy density or for power. The discharge curves of a Marathon battery (12 V, 80 Ah) with an expected life time of 12 years at 20 °C are presented in Fig. 8

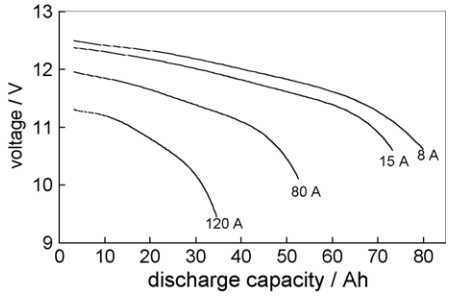

Fig. 8. Discharge curves of 12-V, 80-Ah AGM battery at 20 °C.

It can be seen that even with a rather high current of 120 A, the discharged capacity is about 35 Ah. The discharge time is more than 17 min and the voltage is at a relatively high level for a quite long period. This is a typical characteristic of high-power AGM batteries. This battery type is available as 6-V or 12-V blocks with a capacity range between 30 Ah and 180 Ah at the 10-h discharge rate, and as 2-V cells with capacities between 200 Ah and 500 Ah. It is used for telecommunications systems, as well as, for all applications where a long service life, a high energy density and a medium-to-high discharge power are demanded. The development of this battery range started from older versions of long-life AGM batteries. By improvements in alloys and plate processing, as well as, by some other special design features, it has become possible to increase both the energy and the power density. In parallel, the service life of this battery range can also be extended.

Another range called Sprinter has an expected life time of 10 years and includes 6 V and 12 V batteries with capacities between 60 Ah and 180 Ah. This battery type has a very high discharge power of about 180 Wl^{-1} at the 15 min discharge rate. Sprinter batteries are often used for applications with discharge rates below 1 h down to about 5 min. The power per cell of a Sprinter battery is shown in Fig. 9. The battery has a nominal capacity of 40 Ah at the 10 h rate for discharge time periods between 3 min and 60 min at different cut-off voltages between 1.60 V and 1.90 V per cell. It can be seen that the power available from one cell is more than 2000 W for a discharge time of 5 min.

A further group of very high power batteries, recently developed, includes 12-V batteries between 5 Ah and 85 Ah.

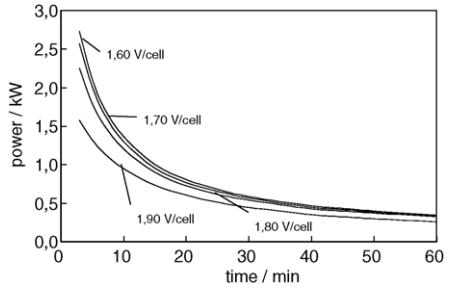

Fig. 9. Discharge power per cell of 40-Ah AGM battery for discharge periods between 3 min and 60 min at different cut-off voltages between 1.60 V and 1.90 V per cell.

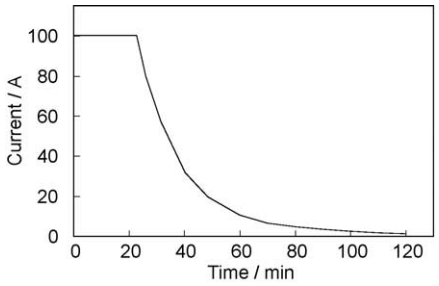

Fig. 10. Fast-charging characteristics of 12-V, 65-Ah AGM battery with current limit of 100 A and voltage of 14.4 V.

These batteries have been optimized to provide power density of 200 Wl^{-1} at the 15 min discharge rate. The typical application is UPS. Due to the optimization towards high power, however the expected life is 5 years and therefore significantly shorter than for the 10-year battery range.

In addition to the high power performance, AGM has also a very good charge-acceptance. The behaviour of a 12-V, 60-Ah AGM battery during charging with 100 A limited by 14.40 V is shown in Fig. 10. The battery was discharged before to 100% DoD. The battery can accept the high current of 100 A over about 20 min. More than 50% of the total capacity is recharged during this time period. After 1 h, the charge current drops down markedly and the battery is recharged to about 90%. It is important to realize that high-power AGM batteries can be recharged very quickly up to a state-of-charge of about 50%, then relatively fast up to 80 to 90% but for the last few percent a significantly longer time is required. This means that after fast charging over 1 h, a slightly lower available capacity has to be accepted. This charge behaviour was measured with AGM batteries having a medium plate thickness. The future trend is to reduce the plate thickness in order to achieve an even higher power performance. This will also be helpful to improve further the charge-acceptance.

There have been some investigations of the temperature increase inside AGM batteries during fast-charging periods [46,47]. The tests showed a significant rise in temperature, but normally this behaviour can be tolerated so that fast charging is an acceptable way to recover quite quickly the battery after a discharge as long as there is a charge voltage limitation. Under certain conditions, however, control by the battery temperature is also needed. With a control of both temperature and charge voltage, the life of AGM batteries will not be reduced by fast charging, as has been proved by some battery tests [48].

The AGM separator has the disadvantage that it does not provide sufficient restraint to prevent expansion of the positive active-mass. This is due to the fact that the glass mat is compressible. There can also be a lack of resilience. A material with similar properties as a glass-mat separator, but which is much less compressible, was proposed recently as an alternative [49]. It is an acid jellifying separator (AJS) that consists of an ultrahigh molecular weight polyethylene with a certain amount of silica inside the pores. Tests with this

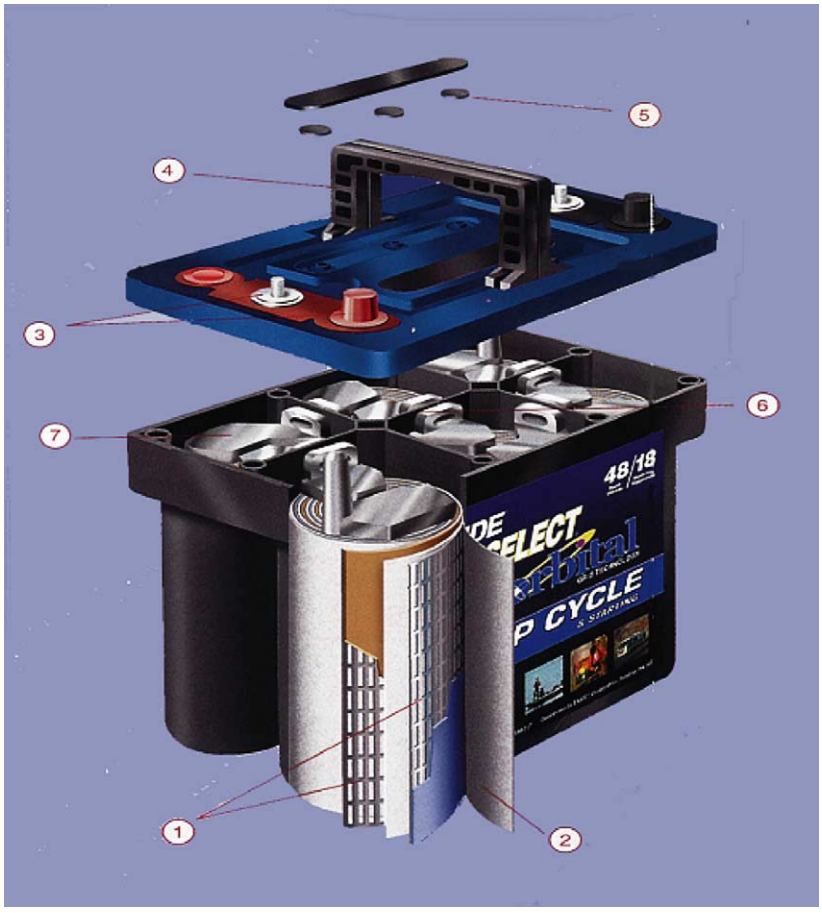

Fig. 11. AGM spiral battery for automotive applications.

separator have shown that there is a very small reduction of the AJS separator thickness with increasing stack pressure [50,51]. The AJS has been compared with AGM and gel in cycle tests. The results are promising and indicate that AJS could be an interesting alternative to AGM for application, where high power and very good cycling performance are required.

6. Orbital design

Besides the traditional design of AGM batteries with flat plates, there is also the option to make cylindrical cells with spiral electrodes and AGM separators. A key point is that the spiral design and the tightly-wound layers of a lead–tin grid make it possible to keep the separator under very high compression. This is rather useful to achieve a combination of an excellent cycle-life and a very high power performance. The thin electrode design provides an active mass surface that is significantly larger than in conventional flat-plate batteries. This reduces the internal electrical resistance and provides exceptional high power [52–54]. A photograph of a 12-V spiral battery with a capacity of 50 Ah – the orbital design – which was developed some years ago as a starter version, is given in Fig. 11.

There have been many investigations of the power capability and charge-acceptance of Orbital batteries at different temperatures and SoCs [55]. The average power supplied at 10 V over 10 s by a 12-V, 50-Ah Orbital battery at different temperatures and SoCs is shown in Fig. 12. At 40 °C and a SoC of 80% or higher, more than 6 kW is provided by the battery. Nevertheless, at all temperatures there is a significant

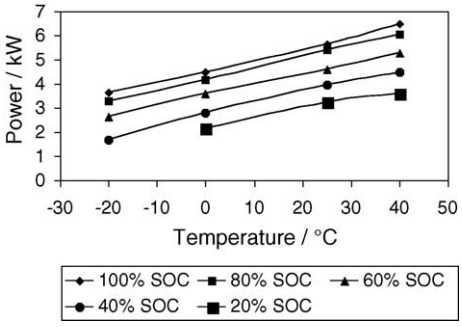

Fig. 12. Discharge power of Orbital battery (12 V, 50 Ah) at different temperatures and SoCs.

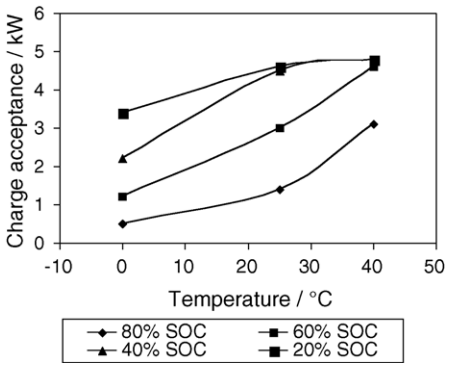

Fig. 13. Charge-acceptance of Orbital battery (12 V, 50 Ah) at different temperatures and SoCs.

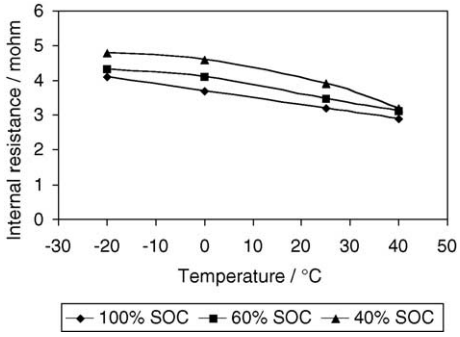

Fig. 14. Internal electrical resistance at discharge of Orbital battery (12 V, 50 Ah) at different SoCs in the temperature range −20 °C to 40 °C.

reduction in power capability with decreasing SoC. At 0 °C and 20% SoC, as well as at −20 °C and 40% SoC, the supplied power is about 2 kW, which is just one-third of that at 40 °C and 80% SoC. Both temperature and a low SoC have a significant impact on power capability. For applications that include the use of the battery at very low temperatures, the SoC should be kept on a relatively high level. It should be realized that any requirement for a good charge-acceptance would result in a conflict, because then it is more favourable to keep the battery at a low SoC.

The average charge-acceptance at 15 V over 5 s at different temperatures and SoCs of the same 12-V, 50-Ah Orbital battery can be seen in Fig. 13. At favourable conditions (high temperature and low SoC), the charge-acceptance is not limited by the battery, but by the power supply equipment. Close to 100% SoC, the charge-acceptance is very poor at all temperatures and is not shown in the diagram. At 0 °C, the charge-acceptance is low unless the battery is nearly fully discharged. At lower temperatures than 0 °C, it is even more difficult to bring a significant amount of power back into the battery.

Thus, from the point of charge-acceptance, temperatures below 0 °C are not favourable and the SoC should be less than 60%. On the other hand, since the power capability is significantly reduced at low temperatures and less than 60% SoC, a compromise must be made to obtain the most suitable SoC, where both power supply and charge-acceptance are at an acceptable level. The problem is the low temperature range. The lower the temperature, the more difficult is the achievement of both acceptable discharge power and charge-acceptance. The problem of low temperature would not be so critical for all applications as during intensive operation a marked increase in battery temperature to a more favourable range can be expected. An alternative would be thermal management, to avoid also excessively high battery temperatures that give reduction in life time.

The exceptional high power capability of Orbital technology can also be seen from the internal electrical resistance that was measured on a 12-V, 50-Ah Orbital battery at different temperatures and SoCs [55]. Data obtained for a discharge after 1 s are presented in Fig. 14. The battery has just about 3 mΩ at 40 °C and even under the unfavourable conditions of −20 °C and 40% SoC, the internal resistance is still below 5 mΩ.

When the internal electrical resistance was measured at charge, after 1 s the results were, as expected, much higher and reflected the well-known experience that the lead–acid system can be discharged with much more power than is possible on recharge. Again, there was no measurement at 100% SoC because of the poor charge-acceptance of a fully-charged battery. There is a significant increase in the electrical resistance at lower temperature or higher SoC, and especially for a combination of both parameters (lower temperature than 20 °C and higher SoC than 60%), as shown in Fig. 15.

For applications where a very good charge-acceptance is required in combination with high discharge power, as for example in a hybrid or mild/soft hybrid in conjunction with regenerative braking, compromises are needed to work within an optimal SoC/temperature range. Such a partial state-of-charge (PSoC) operation requires a certain procedure to bring periodically the battery for a short time back to 100% SoC, otherwise irreversible sulfation cannot be avoided. There have been some detailed investigations about the influence of a high-rate partial state-of-charge (HRPSoC) operation on the life of the negative plate [20,56,57]. By using special additives, a significant improvement can be achieved. During service life, there is some increase in the internal electrical resistances of cells that reduces the high-power performance

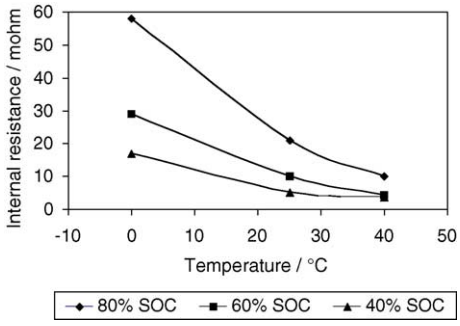

Fig. 15. Internal electrical resistance at charge of Orbital battery (12 V, 50 Ah) at different SoCs in the temperature range 0–40 °C.

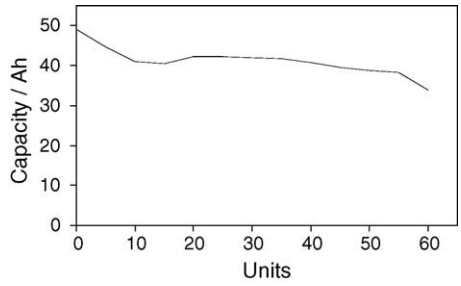

Fig. 16. A 17.5% DoD cycle test of Orbital batteries (12 V, 50 Ah).

due to ageing effects. The regular measurement of internal electrical resistance in combination with OCV measurements is therefore a good way to determine and control the state-of-health of a battery.

There have been studies on orbital batteries (12 V, 50 Ah) subjected to a 17.5% DoD discharge cycling test. This is a special test for automotive batteries. One stage includes a discharge to 50% SoC, then 85 cycles with a 17.5% DoD change, followed by a complete recharge. For flooded types, the requirement is in general six of these stages (510 cycles). The requirement for AGM is three times higher (18 units), taking into account that such batteries have a significantly better cycling performance. Indeed, present high-power AGM types can achieve this number of cycles if they are designed properly. Nevertheless, more than 18 stages appears to be rather difficult for flat-plate AGM batteries with the request for a very high-power capability.

The 17.5% DoD cycling tests on the Orbital batteries showed that 18 stages could be achieved without any problems [56]. Tests were terminated after 18 stages although the batteries were still at a rather high level of capacity. In an additional test, the 17.5% DoD cycling was continued until the battery failed and the very impressive number of 60 stages was achieved [58]. The result, as can be seen in Fig. 16, means that under such duty the Orbital design has a cycling performance that is about three-times that of a flat-plate AGM battery and about ten times that of a flooded battery. There were also some tests where the battery was discharged to 60% SoC and then, subjected to continuous cycling with a rather small change of DoD (1.25%). About 300000 cycles could be achieved under these conditions [56,59].

It should be to realized that the results on Orbital 12-V 50-Ah modules were achieved with a version optimized for a very good cycle-life. A second version has been developed as a power-optimized design with even better results in terms of discharge power and charge-acceptance. Cycle life was slightly worse in comparison with the optimized version, however, although still much better than with conventional flat-plate AGM technology. For application in mild/soft hybrids, life time has a high priority and, therefore, the cycling version would be the better choice.

7. Conclusions

Lead–acid batteries will continue to have by far the major part of the high power battery market. A significant growth in this market is expected for both UPS and automotive applications. Most UPS batteries are already VRLA types whereas on the automotive side nearly all batteries are still of the flooded design. It is expected that future automotive service which, includes stop–start, regenerative braking, soft, mild and full hybrids, will also move towards VRLA. Orbital batteries with spiral electrodes combine excellent cycle-life and very high-power capability, and are promising candidates for future automotive applications.

For UPS applications, there has been a clear tendency to shorter discharge time and higher discharge rates. The requested discharge time is often between 5 min and 15 min and a high supply of power during such periods is the only discharge performance that customers expect from the battery. This means that the battery has to provide a very high power in comparison with the 10-h rate capacity. The current technology is 200 Wl^{-1} at the 15 min rate, but 220 Wl^{-1} is a target which is not unrealistic and prototypes are already available. As a consequence, thinner positive and negative plates have to be used in order to fit more plate couples into a given cell volume.

References

[1] A.I. Attia, D.E. Perrone, ILZRO-Seminar, Orlando, FL, USA, 1989.
[2] E.M. Valeriote, J. Power Sources 28 (1989) 93.
[3] E. Meissner, J. Power Sources 42 (1993) 103.
[4] R. Wagner, J. Power Sources 53 (1995) 153.
[5] G. Barkleit, A. Grahl, M. Maccagni, M. Olper, P. Scharf, R. Wagner, H. Warlimont, J. Power Sources 78 (1999) 73.
[6] R. Kießling, J. Power Sources 19 (1987) 147.
[7] R. Wagner, in: H. Kahlen (Ed.), Batterien, Vulkan, Essen, Germany, 1992.
[8] R. Wagner, VDI Berichte 1058 (1993) 131.
[9] J. Euler, W. Nonnenmacher, Electrochim. Acta 2 (1960) 268.
[10] J. Euler, L. Horn, Electrochim. Acta 10 (1965) 1057.
[11] J. Meiwes, Electrotech. Zeitung 8 (1986) 3.
[12] H. Dominik, G.K. Krämer, B. Voigt, Proceedings of 21th IECEC, San Diego, CA, USA, 1986.
[13] R. Kießling, J. Power Sources 19 (1987) 227.
[14] R. Wagner, J. Power Sources 67 (1997) 163.
[15] K.G. Krämer, Proceedings of Fifth International Conference on Batteries for Energy Storage, Puerto Rico, 1995.
[16] R. Wagner, M. Schroeder, T. Stephanblome, E. Handschin, J. Power Sources 78 (1999) 156.
[17] R. Wagner, J. Electrochem. Soc. 143 (1996) 139.
[18] L.T. Lam, R.H. Newnham, H. Ozgun, F.A. Fleming, J. Power Sources 88 (2000) 92.
[19] M.J. Kellaway, P. Jennings, D. Stone, E. Crowe, A. Cooper, J. Power Sources 116 (2003) 110.
[20] A. Cooper, L.T. Lam, P.T. Mosely, D.A.J. Rand, in: D.A.J. Rand, P.T. Mosely, J. Garche, C.D. Parker (Eds.), Valve-regulated Lead–Acid Batteries, Elsevier, Amsterdam, The Netherlands, 2004.
[21] K. Wen-Hong, J. Power Sources 36 (1991) 155.
[22] Z. Mao, R.E. White, J. Electrochem. Soc. 138 (1991) 1615.

[23] M. Saakes, D. Schellevis, D. van Trier, M. Wollersheim, J. Power Sources 67 (1997) 33.
[24] M. Saakes, E. Kluiters, D. Schmal, S. Mourad, P. ten Have, J. Power Sources 78 (1999) 199.
[25] M. Saakes, C. Kleijnen, D. Schmal, P. ten Have, J. Power Sources 95 (2001) 68.
[26] J. Burbank, J. Electrochem. Soc. 111 (1964) 1112.
[27] H. Giess, in: K.R. Bullock, D. Pavlov (Eds.), Advances in Lead–Acid Batteries, The Electrochemical Society, Pennington, NJ, USA, 1984.
[28] T.G. Chang, in: K.R. Bullock, D. Pavlov (Eds.), Advances in Lead–Acid Batteries, The Electrochemical Society, Pennington, NJ, USA, 1984.
[29] R. Miraglio, L. Albert, A. El Ghachcham, J. Steinmetz, J.P. Hilger, J. Power Sources 53 (1995) 53.
[30] N. Bui, P. Mattesco, P. Simon, J. Steinmetz, E. Rocca, J. Power Sources 67 (1997) 61.
[31] R.D. Prengaman, J. Power Sources 78 (1999) 123.
[32] M.L. Soria, J. Fullea, F. Saez, F. Trinidad, J. Power Sources 78 (1999) 220.
[33] T. Juergens, R.F. Nelson, J. Power Sources 53 (1995) 201.
[34] J.R. Pierson, J. Zagrodnik, R.J. Johnson, J. Power Sources 67. (1997).
[35] R.C. Bhardwaj, J. Power Sources 78 (1999) 130.
[36] M.L. Soria, J. Valenciano, A. Ojeda, G. Raybaut, K. Ihmels, J. Deiters, N. Clement, J. Morales, L. Sanchez, J. Power Sources 116 (2003) 61.
[37] J.K. Whear, W. Böhnstedt, J. Power Sources 116 (2003) 141.
[38] K. Ihmels, W. Böhnstedt, in: D.A.J. Rand, P.T. Mosely, J. Garche, C.D. Parker (Eds.), Valve-regulated Lead–Acid Batteries, Elsevier, Amsterdam, The Netherlands, 2004.
[39] D. Pavlov, J. Power Sources 53 (1995) 9.
[40] N.E. Bagshaw, J. Power Sources 67 (1997) 105.
[41] R. Wagner, P. Scharf, Proceedings of 30th International Symposium on Automotive Technology and Automation, Florence, Italy, 1997.
[42] I. Dreier, F. Saez, P. Scharf, R. Wagner, J. Power Sources 85 (2000) 117.
[43] D. Pavlov, in: D.A.J. Rand, P.T. Mosely, J. Garche, C.D. Parker (Eds.), Valve-regulated Lead–Acid Batteries, Elsevier, Amsterdam, The Netherlands, 2004.
[44] R. Simarro, J. Power Sources 78 (1999) 65.
[45] R. Wagner, in: D.A.J. Rand, P.T. Mosely, J. Garche, C.D. Parker (Eds.), Valve-regulated Lead–Acid Batteries, Elsevier, Amsterdam, The Netherlands, 2004.
[46] H. Giess, Conference Proceedings of INTELEC 2000, Phoenix, AZ, USA, 2000.
[47] P. Häring, H. Giess, J. Power Sources 95 (2001) 153.
[48] R. Wagner, W. Bögel, J.-P. Büchel, Proceedings of 29th International Symposium on Automotive Technology and Automation, Florence, Italy, 1996.
[49] W. Böhnstedt, J. Power Sources 78 (1999) 35.
[50] M. Perrin, H. Döring, K. Ihmels, A. Weiss, E. Vogel, R. Wagner, J. Power Sources 95 (2001) 85.
[51] K. Ihmels, W. Böhnstedt, in: D.A.J. Rand, P.T. Mosely, J. Garche, C.D. Parker (Eds.), Valve-regulated Lead–Acid Batteries, Elsevier, Amsterdam, The Netherlands, 2004.
[52] F. Trinidad, F. Saez, J. Valenciano, J. Power Sources 95 (2001) 24.
[53] F. Trinidad, C. Gimeno, J. Gutierrez, R. Ruiz, J. Sainz, J. Valenciano, J. Power Sources 116 (2003) 128.
[54] J. Valenciano, F. Trinidad, M. Fernandez, J. Power Sources 113 (2003) 318.
[55] J. Valenciano, Internal EXIDE Report, 2004.
[56] J. Valenciano, F. Trinidad, Proceedings of Second European Conference on Alternative Energy Sources for Automobiles, Poitiers, France, 2004.
[57] L.T. Lam, P.T. Moseley, D.A.J. Rand, Batteries and Energy Storage Technology, Summer 2004, 75–78.
[58] J.M. Gonzales, F. Lopez, Internal EXIDE Report, 2004.
[59] M.L. Soria, J. Sainz, J. Valenciano, F. Trinidad, Proceedings of STORE Conference on Storage for Renewable Energies, Aix-en-Provence, France, 2003.